Research Square

Preprints are preliminary reports that have not undergone peer review.
They should not be considered conclusive, used to inform clinical practice,
or referenced by the media as validated information.

# Rethinking Radical Quantification Methods in VUV/UV Water Treatment Process: Alcohol Scavenging and Probe-Model Combining Strategy

**Lan Li**
Harbin Institute of Technology
**Qiaoxia Han**
Harbin Institute of Technology
**Boqiang Li**
Tongji University
**Longjie Cheng**
Harbin Institute of Technology
**Baiyang Chen**
chen.baiyang@hit.edu.cn
Harbin Institute of Technology

**Research Article**

**Keywords:** Probing methods, Scavenging methods, Radical concentration and contribution, Kinetic modeling, Water matrix

**Posted Date:** November 3rd, 2026

**DOI:** https://doi.org/10.21203/rs.3.rs-11277963/v1

**License:** This work is licensed under a Creative Commons Attribution 4.0 International License.
Read Full License

**Additional Declarations:** No competing interests reported.

# Abstract

The use of vacuum ultraviolet (VUV)/ultraviolet (UV) technology for water pollutant degradation has grown rapidly in recent years; however, distinguishing the roles of the radicals generated in this process remains difficult and sometimes even methodologically unsound. To address this issue, this study evaluated three methods commonly used for radical determination in advanced oxidation processes (AOPs) and optimized them through rational design choices. The results show that the use of alcohol quenchers generated additional amounts of $H_2O_2$, which can perturb the chemistry of the scavenged system and bias the role of HO•. Increasing solution pH inhibited $H_2O_2$ formation significantly from isopropanol and tert-butanol but mildly from methanol, and lowering dissolved oxygen to 2.5 mg/L by purging nitrogen gas continuously reduced $H_2O_2$ formation dramatically. Collectively, these results indicate that using alcohols is not a reliable choice for radical quantification under practical conditions. Instead, the reliability of radical determination and contribution analysis can be improved by combining kinetic modeling with the probing method, since a model depends strongly on the quantity and quality of input reactions and rate constants and probing experiments can help calibrate those data used for modeling. By combining both, this study found that the VUV/UV process was essentially governed by scavenging of primary radicals and formation of secondary radicals in water matrices, and the types and concentrations of radicals evolved dynamically over time. Collectively, this study provides fundamental insights into methods for determining radicals in complex systems containing multiple radical species.


# 1. Introduction

Vacuum ultraviolet/ultraviolet (VUV/UV) treatment has attracted increasing attention in water treatment because it can promote contaminant degradation without the addition of external oxidants. Unlike conventional UV processes, VUV irradiation can directly photolyze water and initiate the formation of multiple reactive species. A VUV/UV lamp emits light at both 185 and 254 nm and the former can directly photolyze water to generate oxidizing radicals such as hydroxyl radicals (HO•) and reducing species such as hydrogen atoms (H•), together with hydrated electrons ($e_{aq}^-$), while hydrogen peroxide ($H_2O_2$) can also be formed as a secondary oxidant [1, 2].

$H_2O \rightarrow HO\bullet + H\bullet$ (1)

$H_2O \rightarrow HO\bullet + H^+ + e_{aq}^-$ (2)

However, although earlier studies assumed that radical concentrations remain constant throughout water treatment during VUV/UV [3], $H_2O_2$ can be generated continuously photolysis [4], thereby elevating the concentration of HO• over time and confounding attempts to treat its role as invariant. In addition, water constituents such as anions and natural organic matter (NOM) can often compromise the performance of the VUV/UV process by scavenging primary radicals and forming secondary radicals [5]. For example, HO• reacts with $HCO_3^-$ to yield $CO_3\bullet^-$, with $Br^-$ to yield Br• and $Br_2\bullet^-$, and with $Cl^-$ to yield Cl•

and $Cl_2^{\bullet-}$ [5]. Although all of these reactive species (RSs) can degrade certain aqueous pollutants during the VUV/UV process, their contributions were often attributed to HO• solely because the concentrations of $e_{aq}^-$ and H• are negligible under high dissolved oxygen (DO) conditions and $H_2O_2$ formation is limited [6, 7]. Therefore, a reliable framework for detecting all radicals is essential for understanding the practical application of VUV/UV technology [8].

To date, the major methods for identifying and quantifying radicals include: (1) spectroscopic methods such as electron spin resonance/electron paramagnetic resonance (EPR) and laser-induced fluorescence; (2) probing methods using nitrobenzene (NB) and/or para-chlorobenzoic acid (p-CBA); (3) scavenging methods using methanol or tert-butyl alcohol (TBA); and (4) kinetic modeling with software such as Kintecus [7, 8]. Among these, EPR instrumentation and its consumables are costly, and, more importantly, EPR primarily provides evidence for the presence rather than the quantity of radicals; it is therefore less quantitative [8, 9].

In contrast, scavenging and probing methods are widely adopted because they are simple to perform and easy to monitor [9, 10]. Among scavengers, alcohols have been widely used in the VUV/UV process [11, 12]. By comparing the degradation kinetics of a target pollutant before and after quenching, the contribution of HO• can be inferred [13]. However, quenching HO• with alcohols could generate substantial amounts of $H_2O_2$ under oxygen-rich conditions, which in turn can lead to additional HO• formation [11] and perturb the chemistry of the scavenged system. Consequently, the degradation observed after alcohol addition may not simply represent a condition in which HO• has been removed, potentially biasing scavenging-based radical attribution. Importantly, enhanced $H_2O_2$ formation during VUV irradiation of methanol-containing aqueous solutions has already been reported by Robl et al. [14]. However, the implications of this alcohol-induced chemistry for quantitative radical attribution in VUV/UV systems remain insufficiently resolved. Moreover, because the VUV/UV process can potentially generate a higher concentration of HO• than the UV/$H_2O_2$ process, the extent to which different alcohol scavengers promote $H_2O_2$ accumulation under VUV/UV conditions and thereby perturb the intended scavenging chemistry warrants systematic evaluation. In addition, because some operational factors affect the performance of the VUV/UV process [1, 2], their effects on alcohol-induced $H_2O_2$ formation should also be considered when assessing the applicability of scavenging methods under different reaction conditions.

Probing methods are commonly used to quantify radicals by monitoring the decay of dosed probe compounds, which are usually selective to certain radical(s) only [8, 13]. Because probe dosages are typically far lower than those of target pollutants, probing methods do not appreciably perturb the system [10], which is desirable. The second-order rate constants (k) for radical-pollutant reactions can be either obtained from literature [15, 16] or determined experimentally by laser flash photolysis [17, 18]. Once the relevant k values are known, the contribution of a radical to pollutant degradation can be estimated by multiplying its concentration by the corresponding k value [13]. The shortcomings of this method, however, lie in two aspects: one is the difficulty of obtaining all k values for numerous pollutants

reacting with various radicals, and the other is the potential for misattribution when multiple reactive radicals are present since different radicals may degrade probes and pollutants separately, while the removal of a pollutant may be mistakenly attributed to a certain radical that degrades the selected probe.

As for kinetic modeling, its results must be validated against experimental data that cover all relevant reactions and species, so that its application is generally limited to well-characterized systems [19, 20]. Otherwise, the reliability of kinetic modeling depends on the kinetics of all relevant reactions, which typically require a substantial amount of input data [20]. Therefore, model predictions become increasingly uncertain when important reactions, rate constants, or time-dependent matrix effects are insufficiently characterized [19]. However, model validation has sometimes been performed without sufficient rigor. For instance, researchers often justified a model solely by the evolution of a single compound rather than the trends of multiple reactants, intermediates, and products [21, 22]. Because adjusting different modeling parameters may produce the same model behavior, erroneous parameter sets may be obtained if agreement between experimental and modeled data was achieved by chance [23].

To clarify these methodological issues and establish a cross-evaluation framework, the present study assesses three radical-determination methods for the VUV/UV process to elucidate the roles of different radicals in pollutant degradation with or without the addition of selected anions and dissolved organic matter (DOM). The objectives are pursued through the following efforts: (1) to evaluate the potential interference associated with alcohol-based scavenging for radical quantification; (2) to compare radical evolution during the degradation of typical pollutants obtained experimentally with that obtained using an approach combining probing and modeling methods; and (3) to differentiate the contributions of individual radicals to pollutant degradation under complex water conditions. Overall, this study provides a framework for cross-evaluating scavenging, probing, and kinetic modeling approaches in systems containing multiple coexisting radicals.

## 2. Materials and methods

# 2.1 Chemical reagents

All reagents were of analytical grade. Methanol (MeOH), ethanol (EtOH), 1-propanol (NPA), 1-butanol (NBA), 2-propanol (IPA), 2-methylpropan-1-ol (IBA), and 2-methylpropan-2-ol (TBA) were obtained from Aladdin Inc. (China). Nitrobenzene (NB), 1,4-dimethoxybenzene (DMOB), para-chlorobenzoic acid (p-CBA), carbamazepine (CBZ), metronidazole (MTZ), phenol, and hydroquinone (HQ) (purity > 98%) were purchased from Adamas. Sodium chloride (NaCl), sodium bromide (NaBr), and sodium bicarbonate ($NaHCO_3$), used as the sources of $Cl^-$, $Br^-$, and $HCO_3^-$, respectively, were purchased from Aladdin Inc. (China). DOM was prepared using a fulvic acid standard. Sodium hydroxide (NaOH; Aladdin Inc., China) was used to adjust the solution pH. All solutions were prepared with ultrapure water (18.2 MΩ·cm). A 1.0 mol/L $H_2O_2$ stock solution was prepared weekly from 30% (w/w) $H_2O_2$ and stored at 4°C.

## 2.2 Experimental procedure

All reactions were performed in a cylindrical stainless-steel photoreactor (length 320 mm, inner diameter 60 mm, working volume 450 mL). A 23 mm quartz sleeve housed a 12 W low-pressure mercury lamp emitting at 185 and 254 nm. The reactor design is shown in Figure S1. Using $H_2O_2$ as an actinometer, the light intensity and optical path length were determined to be $1.89 \times 10^{-5}$ Einstein $L^{-1}$ $s^{-1}$ and 1.26 cm, corresponding to a photon flux of $2.37 \times 10^{-8}$ Einstein $cm^{-2}$ $s^{-1}$ and a UV intensity of 11.2 mW $cm^{-2}$, respectively.

At room temperature (25 ± 1°C), the selected alcohols at 0.1, 1, 10, and 20 mM were added separately to ultrapure water and then transferred to the continuously stirred photoreactor. Except for the low-DO experiments, the reactor was open to air during the experiments to permit continuous $O_2$ exchange at the water surface. The initial pH and DO of the ultrapure water were approximately 6.4 and 8.5 mg/L, respectively. The pH was adjusted to 8 and 10 with NaOH only, to avoid introducing other ions that could interfere with subsequent analysis. For the low-DO experiments, the solution was purged with $N_2$ continuously until the DO reached 2.5 mg/L and then irradiated in a sealed photoreactor to minimize $O_2$ re-entry, while 8.5 mg/L represented the air-saturated condition.

For experiments on probe and target-compound degradation, NB, DMOB, p-CBA, CBZ, MTZ, phenol, and HQ (each at 0.5 μM) were degraded by the VUV/UV process in ultrapure water, DOM-containing water (5 mg-C/L), or synthetic water containing DOM (5 mg-C/L), $Cl^-$ (2 mM), $Br^-$ (10 μM), and $HCO_3^-$ (2 mM), depending on the experiment. Direct UV control experiments were additionally conducted for NB and p-CBA (0.5 μM) to evaluate their direct photolysis. Blank and replicate tests were performed for all experiments. For the time-resolved NB probing experiments, the water matrix was first irradiated for a predetermined period (0, 10, 20, or 30 min), after which fresh NB was introduced to a final concentration of 0.5 μM. NB decay was then monitored over the subsequent 10-min interval. Thus, the intervals of 0–10, 10–20, 20–30, and 30–40 min represented independent probing experiments rather than continuous irradiation of a single NB dose.

## 2.3 Analytical methods

In this study, $H_2O_2$ was analyzed by ion chromatography (IC) following published procedures [24]. The pH was measured with a pH meter (Thermo Fisher, model 8103BN). DO was measured with an optical sensor (Starter 400D, Ohaus, USA). The concentrations of NB, CBZ, p-CBA, MTZ, DMOB, phenol, and HQ were determined by high-performance liquid chromatography (HPLC; LC3200, Wayeal, China) equipped with a C18 column (150 mm × 4.2 mm, 5 μm; JK Chemical Co., China) and a UV diode-array detector (DAD).

The mobile phases were mixtures of water and acetonitrile at volume ratios of 40:60 (NB and DMOB), 50:50 (MTZ), 20:80 (CBZ), and mixtures of 1% phosphoric acid and acetonitrile at volume ratios of 50:50 (p-CBA), 70:30 (HQ), and 40:60 (phenol). All eluents were delivered at 0.5 mL/min and 30°C. The

detection wavelengths were 268, 225, 316, 283, 236, 292, and 215 nm for NB, DMOB, MTZ, CBZ, p-CBA, phenol, and HQ, respectively. Each test was performed in duplicate, and the results are reported as mean ± absolute deviation.

## 2.4 Radical determination and kinetic modeling

The Kintecus (Version 2025) software was used to simulate contaminant and probe degradation and to estimate radical concentrations during the VUV/UV process. The reactions and rate constants incorporated in the models were taken from the literature or calculated in this study, as summarized in Table S1. The complete reaction network, photochemical inputs, initial conditions, and matrix-specific model assumptions used for the simulations are provided in Text S1 and Table S1. Because information on certain reaction intermediates and their radical reactivities remains limited, the model includes the parent compounds and reactive species for which kinetic information was available and should therefore be regarded as a mechanistic representation rather than an exhaustive description of the reaction system. The HO• exposure was calculated using Eq. (1) in Text S1, and the corresponding HO• concentration was obtained using Eq. (2). The modeled HO• concentrations were averaged over the same reaction intervals for comparison with the experimentally determined values. In complex water matrices, the cumulative contributions of HO•, Cl•, $Cl_2^{\bullet -}$, Br•, $Br_2^{\bullet -}$, $CO_3^{\bullet -}$, and UV to micropollutant degradation were calculated from the pathway-specific degradation rates using Eqs. (3)–(8) in Text S1 and expressed as percentages of the initial micropollutant concentration.

# 3 Results and discussion

## 3.1 Evaluation of scavenging method

### 3.1.1 $H_2O_2$ formation with and without alcohols

Figure 1 shows $H_2O_2$ formation in the VUV/UV process in the presence and absence of alcohols. Without alcohol, the $H_2O_2$ concentration reached only 3.0 μM over the photolysis period, probably because HO• generated by VUV cleavage of $H_2O$ can self-recombine to form $H_2O_2$ [1, 4]. In contrast, a markedly higher amount of $H_2O_2$ was produced in the presence of 1 mM MeOH (101.8 μM), IPA (99.5 μM), EtOH (93.9 μM), IBA (88.1 μM), NPA (80.5 μM), TBA (69.5 μM), or NBA (60.7 μM), demonstrating that chain reactions between alcohols and HO• under DO-rich conditions could generate additional $H_2O_2$ (Reactions 1–3) [11].

HO-RH + HO• → HO-R• + $H_2O$ k = $6.2 \times 10^8 - 4.2 \times 10^9$ $M^{-1}$ $s^{-1}$ (1)

HO-R• + $O_2$ → HO-ROO• k ≈ $4.9 \times 10^9$ $M^{-1}$ $s^{-1}$ (2)

2 HO-ROO• → HO + other products k ≈ 2.1 × 10 M s (3)

The differences in $H_2O_2$ yields among alcohols can be attributed to two factors: (1) the differing rates of reaction between individual alcohols and HO• [25], which give distinct $H_2O_2$ formation rates (Table S2); and (2) the differing reducing abilities of alcohol radicals (HO-R•), which consume $H_2O_2$ at different rates and to different extents [26, 27]. For example, the redox potentials of the IPA (− 1.37 V), TBA (− 1.25 V), and MeOH (− 1.07 V) radicals vary in the same order as their residual $H_2O_2$ levels at 90 min: IPA (1.7 μM) < TBA (13.1 μM) < MeOH (58.6 μM).

Note that the minimum $H_2O_2$ yield (60.7 μM from NBA) was still far above the 10 μM $H_2O_2$ typically dosed in UV/$H_2O_2$ systems [11], demonstrating that alcohol addition substantially altered the reaction chemistry of the VUV/UV system. Because $H_2O_2$ can serve as a precursor of HO•, the alcohol-amended system cannot be regarded simply as an HO•-quenched condition. Consequently, alcohol-induced $H_2O_2$ formation may bias scavenging-based estimation of the HO• contribution, although the direction and magnitude of this bias cannot be determined from $H_2O_2$ formation alone. Accordingly, the use of alcohols as quenchers for radical quantification in the VUV/UV process should be interpreted with caution.

3.1.2 Effects of influencing factors on $H_2O_2$ formation

To optimize the quenching procedure and if possible, avoid above issues, Fig. 2a, Fig. S2a, and Fig. S3a present the effects of several operational factors on $H_2O_2$ formation. These figures show that raising the DO concentration from 2.5 ± 0.5 to 8.5 ± 0.5 mg $L^{-1}$ markedly increased $H_2O_2$ production. To suppress additional $H_2O_2$ formation and reduce its interference with HO• scavenging, scavenging tests should be conducted under low-DO conditions, which are very difficult to maintain without continuous $N_2$ bubbling or in a sealed system [1].

Figure 2b, Fig. S2b, and Fig. S3b show that the maximum $H_2O_2$ concentrations of MeOH, IPA, and TBA within 20 min decreased—from 100.5, 99.5, and 69.5 μM to 50.0, 20.3, and 14.7 μM, respectively—as the pH was raised from 6.4 to 10.0. This inhibition may be partly due to the reduced reactivity of HO• under alkaline conditions [28] and partly to the additional consumption of organic peroxyl radicals (HO-ROO•), key intermediates in $H_2O_2$ formation (Reaction 4), by $OH^-$ [29, 30]. In contrast to IPA and TBA, MeOH showed a weaker pH dependence in $H_2O_2$ formation (Fig. 2), indicating that high pH suppresses $H_2O_2$ generation more strongly for IPA and TBA than for MeOH.

$$\text{HO-ROO}\bullet + OH^- \rightarrow \text{HR}(=O)H + O_2\bullet^- + H_2O \qquad k \approx (4.0–5.2) \times 10^9\ M^{-1}\ s^{-1} \qquad (4)$$

As shown in Fig. 2c, Fig. S2c, and Fig. S3c, no clear trend emerged in the maximum $H_2O_2$ concentration as the initial alcohol dose increased from 0.1 to 20.0 mM. This suggests that, although higher alcohol concentrations enhance HO• scavenging, alcohols also absorb 185 nm VUV photons [31] and thereby reduce water photolysis at 185 nm and the subsequent formation of HO•. Overall, both the dose and the type of alcohol used as a quencher must be selected carefully to minimize side effects.

## 3.2 Evaluation of probing and modeling methods

### 3.2.1 Validation of modelling data with probing method

To track radical evolution, 0.5 μM NB was used as a selective probe and freshly introduced at different irradiation intervals to determine the HO• concentration in each interval. Direct UV photolysis of NB was negligible under the experimental conditions (Fig. S5) and was therefore neglected in the calculation of HO• exposure. Kintecus models were constructed and validated against the experimental results [5].

Based on NB degradation in synthetic water containing DOM (5 mg-C/L) at different time intervals (0–10, 10–20, 20–30, and 30–40 min; Fig. S4), the HO• concentration were $1.44 \times 10^{-12}$, $4.90 \times 10^{-12}$, $7.18 \times 10^{-12}$, and $1.01 \times 10^{-11}$ M, respectively. The Kintecus model simulated this evolution of HO• well (Fig. S4), indicating that it captures all relevant reactions and reactants in this process.

Moreover, the reliability of the model was confirmed by simulating the degradation of representative compounds (i.e., DMOB and CBZ) under different water-quality conditions (Fig. 3). It should be noted that the 185 nm absorbance of the added aqueous matrix could significantly affect the accuracy of the modeling. For example, 1 mM $Cl^-$ has a 185 nm molar absorption coefficient as high as 3300 $M^{-1}$ $cm^{-1}$ [31, 32], so the effect of $Cl^-$ absorption at 185 nm was incorporated into the model. Accounting for this absorption substantially altered the modeled cumulative pathway contributions (Fig. S7). As shown in Fig. 3, the half-lives of pollutant degradation (200–300 s) in a complex matrix containing both DOM (5 mg-C/L) and typical anions (e.g., 2 mM $Cl^-$, 10 μM $Br^-$, and 2 mM $HCO_3^-$) were much longer than those in DOM-only water (5 mg-C/L; 90–120 s), which in turn were longer than those in pure water (15–20 s). Therefore, although some studies suggest that the formation of secondary radicals might facilitate contaminant degradation [5], the complexity of aqueous constituents in the selected water matrix actually reduced the overall degradation rate constants [1].

To further validate the model, 0.5 μM NB, p-CBA, and MTZ were introduced separately into DOM-containing water (5 mg-C/L), and their degradation profiles were compared with the corresponding model simulations (Fig. S6). After this validation, the modeling approach was applied to obtain radical concentrations in different aqueous matrices, including the complex matrix containing DOM (5 mg-C/L), $Cl^-$ (2.0 mM), $Br^-$ (10.0 μM), and $HCO_3^-$ (2.0 mM).

### 3.2.2 Determination of radical concentrations

Figure 4c shows the evolution of key radicals in water containing DOM (5 mg-C/L), $Cl^-$ (2 mM), $Br^-$ (10 μM), and $HCO_3^-$ (2 mM) during the VUV/UV process. At 40 min, the modeled radical concentrations were obtained and ranked as follows: $CO_3^{\bullet -}$ ($8.71 \times 10^{-12}$ M) > HO• ($4.79 \times 10^{-13}$ M) > $Br_2^{\bullet -}$ ($3.11 \times 10^{-13}$ M) > Br• ($2.98 \times 10^{-14}$ M) > H• ($7.32 \times 10^{-15}$ M) > $e_{aq}^-$ ($1.04 \times 10^{-15}$ M) > $Cl_2^{\bullet -}$ ($5.83 \times 10^{-16}$ M) > Cl• ($8.94 \times 10^{-18}$ M). $CO_3^{\bullet -}$ prevailed because it was generated through multiple carbonate/bicarbonate reaction

pathways and had comparatively limited scavenging pathways (Table S1). In contrast, Cl• and $Cl_2^{\bullet-}$ react rapidly with secondary radicals and ions, giving them low concentrations. For instance, as Cl• and $Cl_2^{\bullet-}$ react with $Br^-$ and $HCO_3^-$ to form $Br_2^{\bullet-}$ and $CO_3^{\bullet-}$ (Reactions 5–8 and 12–17), the concentrations of Br• and $Br_2^{\bullet-}$ exceed those of Cl• and $Cl_2^{\bullet-}$. Notably, HO• and $CO_3^{\bullet-}$ increased gradually during irradiation, whereas Br• and $Br_2^{\bullet-}$ decreased slightly, from $3.96 \times 10^{-14}$ and $4.05 \times 10^{-13}$ M at 5 s to $2.98 \times 10^{-14}$ and $3.11 \times 10^{-13}$ M after 40 min, respectively. H• remained nearly constant, while $e_{aq}^-$, Cl•, and $Cl_2^{\bullet-}$ decreased slightly. Compared with the HO• concentration in DOM-only synthetic water ($1.87 \times 10^{-12}$ M; Fig. 4b), the HO• concentration in water containing both DOM and ions ($4.79 \times 10^{-13}$ M) was ~ 74% lower. This decrease reflects the consumption of HO• by coexisting ions and its conversion into secondary radicals (Reactions 11 and 18–26). Overall, the coexistence of multiple water constituents markedly alters the types and levels of radicals, leading to dominant mechanisms that differ from those observed in ultrapure water.

| | | |
|---|---|---|
| **$Cl^{\bullet} + CO_3^{2-} \rightarrow Cl^- + CO_3^{\bullet -}$** | **$5.00 \times 10^8\ M^{-1}\ s^{-1}$** | **(5)** |
| $Cl^{\bullet} + HCO_3^- \rightarrow Cl^- + CO_3^{\bullet -} + H^+$ | $2.20 \times 10^8\ M^{-1}\ s^{-1}$ | (6) |
| $Cl_2^{\bullet -} + CO_3^{2-} \rightarrow 2Cl^- + CO_3^{\bullet -}$ | $1.60 \times 10^8\ M^{-1}\ s^{-1}$ | (7) |
| $Cl_2^{\bullet -} + HCO_3^- \rightarrow 2Cl^- + CO_3^{\bullet -} + H^+$ | $8.00 \times 10^7\ M^{-1}\ s^{-1}$ | (8) |
| $BrO^- + CO_3^{\bullet -} \rightarrow CO_3^{2-} + BrO^{\bullet}$ | $4.30 \times 10^7\ M^{-1}\ s^{-1}$ | (9) |
| $CO_3^{\bullet -} + CO_3^{\bullet -} \rightarrow$ other products | $3.00 \times 10^7\ M^{-1}\ s^{-1}$ | (10) |
| $HO^{\bullet} + CO_3^{\bullet -} \rightarrow$ other products | $3.00 \times 10^9\ M^{-1}\ s^{-1}$ | (11) |
| $Cl_2^{\bullet -} + Br^- \rightarrow ClBr^{\bullet -} + Cl^-$ | $4.00 \times 10^9\ M^{-1}\ s^{-1}$ | (12) |
| $Cl^{\bullet} + Br^- \rightarrow ClBr^{\bullet -}$ | $1.20 \times 10^{10}\ M^{-1}\ s^{-1}$ | (13) |
| $Br^{\bullet} + Cl^- \rightarrow ClBr^{\bullet -}$ | $1.00 \times 10^8\ M^{-1}\ s^{-1}$ | (14) |
| $ClOH^{\bullet -} + Br^- \rightarrow ClBr^{\bullet -} + OH^-$ | $1.00 \times 10^9\ M^{-1}\ s^{-1}$ | (15) |
| $BrOH^{\bullet} + Cl^- \rightarrow ClBr^{\bullet -} + OH^-$ | $1.90 \times 10^8\ M^{-1}\ s^{-1}$ | (16) |
| $ClBr^{\bullet -} + Br^- \rightarrow Br_2^{\bullet -} + Cl^-$ | $8.00 \times 10^9\ M^{-1}\ s^{-1}$ | (17) |
| $HO^{\bullet} + Cl^- \rightarrow ClOH^{\bullet -}$ | $4.30 \times 10^9\ M^{-1}\ s^{-1}$ | (18) |
| $ClBr^{\bullet -} + HO^{\bullet} \rightarrow BrCl + OH^-$ | $1.00 \times 10^9\ M^{-1}\ s^{-1}$ | (19) |
| $HO^{\bullet} + Br^- \rightarrow BrOH^{\bullet -}$ | $1.10 \times 10^{10}\ M^{-1}\ s^{-1}$ | (20) |
| $HOBr + HO^{\bullet} \rightarrow BrO^{\bullet} + H_2O$ | $2.00 \times 10^9\ M^{-1}\ s^{-1}$ | (21) |
| $BrO^- + HO^{\bullet} \rightarrow BrO^{\bullet} + OH^-$ | $4.50 \times 10^9\ M^{-1}\ s^{-1}$ | (22) |
| $HO^{\bullet} + DOM \rightarrow$ other products | $2.95 \times 10^8\ M^{-1}\ s^{-1}$ | (23) |
| $HO^{\bullet} + CO_3^{2-} \rightarrow CO_3^{\bullet -} + OH^-$ | $3.90 \times 10^8\ M^{-1}\ s^{-1}$ | (24) |
| $HO^{\bullet} + HCO_3^- \rightarrow CO_3^{\bullet -} + H_2O$ | $8.60 \times 10^6\ M^{-1}\ s^{-1}$ | (25) |
| $HO^{\bullet} + H_2CO_3 \rightarrow CO_3^{\bullet -} + H_2O + H^+$ | $1.00 \times 10^6\ M^{-1}\ s^{-1}$ | (26) |

## 3.3 Modeling the contributions of radicals to pollutant degradation

Using the obtained radical concentrations and the corresponding second-order rate constants (k) used in the model with the micropollutants, together with the pseudo-first-order rate constants for direct UV photolysis, the cumulative contributions to micropollutant degradation were calculated. As shown in Fig. 5, for CBZ degradation in the complex system, the contribution order was HO• > UV > Br• > $Br_2^{\bullet-}$ > $CO_3^{\bullet-}$ throughout the investigated period. For DMOB degradation, HO• was the dominant contributor, followed by $CO_3^{\bullet-}$, with the contribution order as HO• > $CO_3^{\bullet-}$ > Br• > UV > $Br_2^{\bullet-}$. This indicates that Cl• and $Cl_2^{\bullet-}$ made negligible contributions to the degradation of these pollutants, whereas the relative importance of UV, Br•, and $CO_3^{\bullet-}$ depended strongly on the target pollutant.

It is worth noting that the cumulative contributions of all pathways increased with reaction time as pollutant removal proceeded, so that their relative shares of total degradation changed over time. The relative share of HO• increased markedly for both CBZ and DMOB, whereas that of $CO_3^{\bullet-}$ increased slightly. The share of UV decreased, while those of Br• and $Br_2^{\bullet-}$ decreased only slightly overall. These changes are mainly due to the declining concentrations of Br• and $Br_2^{\bullet-}$and the gradual increase in HO• and $CO_3^{\bullet-}$ concentrations, whereas the pseudo-first-order rate constant for direct UV photolysis of each pollutant remained constant over time. Among the secondary radicals, Br• was the major contributor to CBZ degradation, whereas $CO_3^{\bullet-}$ was the major contributor to DMOB degradation. The contributions of Cl• and $Cl_2^{\bullet-}$ were negligible.

Overall, these insights gained from the dynamics of radical contributions can not only deepen our understanding of pollutant degradation mechanisms but also guide the development of efficient and targeted processes for real-world applications. Future studies should optimize operational parameters to maximize the effectiveness of the VUV/UV process across diverse water treatment scenarios.

# 4. CONCLUSIONS

This study evaluated the scavenging, probing, and kinetic modeling methods for determining radicals in the VUV/UV process under various conditions. Alcohol-based quenching was shown to generate substantial additional $H_2O_2$ via chain reactions with HO•, so that this method can misrepresent the role of HO• and should therefore be used with caution, particularly under oxygen-rich conditions. The probing and kinetic modeling methods, when used together and validated using multiple probes and compounds, provided a more robust tool for tracking radical evolution, meanwhile it should be remaindered that the modeling accuracy depends strongly on the completeness and quality of reaction inputs and must account for the 185 nm absorbance of the aqueous matrix. In complex water containing DOM and anions, the concentrations and pathway contributions of reactive species evolved dynamically with

reaction time. HO• remained the major contributor to the degradation of both CBZ and DMOB, whereas the contributions of secondary radicals were strongly pollutant dependent, with Br• contributing substantially to CBZ degradation and $CO_3^{\bullet -}$ playing a major secondary-radical role in DMOB degradation. These results demonstrate that radical concentration alone cannot be used to infer its importance in pollutant degradation, because the contribution of each radical also depends on its reaction rate constant with the target pollutant. Although this framework is somehow complicated and tedious, we still recommend combining probing and modeling methods to achieve reliable determination of coexisting radicals and their time-dependent contributions in complex treatment systems such as the VUV/UV process.

Notably, practical implementation of the framework must also account for many other factors such as disinfection-by-product formation, residual oxidant effects, toxicity of transformation products, and site-specific chemical and energy costs. Beyond this study, the framework also requires further validation against realistic samples with additional water constituents (e.g., nitrate, sulfate, bromide). Future work can either extend it by incorporating more detailed theoretical and practical considerations and or stream or simplify certain steps to reduce experimental burden. We anticipate that adopting such a framework will foster more rigorous and generalizable kinetic modeling of the VUV/UV process and, in turn, more reliable translation of this process from the laboratory to full-scale water treatment.

## Declarations

# Clinical trial number

Not applicable.

**Ethics, Consent to Participate, and Consent to Publish declarations**

Not applicable.

# Funding

This study is financially supported by the State Key Laboratory of Urban-Rural Water Resource and Environment (Harbin Institute of Technology) (No. 2024TS09), the Shenzhen Science and Technology Innovation Committee (SYSPG20241211173609007), and the National Natural Science Foundation of China (51978194).

# Author Contribution

L.L.: Methodology, Modeling, Formal analysis, Visualization, Writing – original draft. Q.H.: Investigation, Modeling, Formal analysis, Writing – original draft. B.L.: Methodology, Validation, Supervision. L.C.:

Methodology, Validation, Supervision. B.C.: Conceptualization, Supervision, Project administration, Funding acquisition, Writing – review & editing. All authors reviewed and approved the final manuscript.

# Data Availability

The datasets generated and/or analyzed during the current study are available from the corresponding author on reasonable request.

## References


1. Zhang H, Sun W, Zhang J, Ma J. Vacuum-ultraviolet based advanced oxidation and reduction processes for water treatment. J Hazard Mater. 2024;471:134432.
2. Zhang B, Jiang G, Shi W, Xue Y, Sun W. Vacuum-ultraviolet technology photolysis of aqueous reaction systems for organic pollutants abatement. Chin Chem Lett. 2026;37(2):111371.
3. Wols BA, Hofman-Caris CHM. Review of photochemical reaction constants of organic micropollutants required for UV advanced oxidation processes in water. Water Res. 2012;46(9):2815–27.
4. Zhang Q, Wang L, Chen B, Chen Y, Ma J. Understanding and modeling the formation and transformation of hydrogen peroxide in water irradiated by 254 nm ultraviolet (UV) and 185 nm vacuum UV (VUV): effects of pH and oxygen. Chemosphere. 2020;244:125483.
5. Li B, Pan H, Chen B. A review of factors affecting the formation and roles of primary and secondary reactive species in UV254-based advanced treatment processes. Water Res. 2023;244:120537.
6. Wu Z, Shang C, Wang D, Zheng S, Wang Y, Fang J. Rapid degradation of dichloroacetonitrile by hydrated electron ($e_{aq}^-$) produced in vacuum ultraviolet photolysis. Chemosphere. 2020;256:126994.
7. Wang C, Wang X, Du J, Deng R, Ren B, Zhou S, et al. Vacuum UV-based processes for water and wastewater purification: from unitary to multicomponent systems. Water Res. 2025;275:123175.
8. Li W, Song G, Jing J, Ren X, Zhang C, Oturan MA, et al. Identification and quantification of reactive species in aqueous medium during application of advanced oxidation processes: a critical review. Chem Eng J. 2024;500:156698.
9. Huang B, Wu Z, Zhang J, Shi Y, He CS, Xiong Z, et al. Is the choice of quencher appropriate for exploring reactive oxygen species in advanced oxidation processes? Chin Chem Lett. 2026;37(3):111537.
10. Hübner U, Spahr S, Lutze H, Wieland A, Rüting S, Gernjak W, et al. Advanced oxidation processes for water and wastewater treatment—guidance for systematic future research. Heliyon. 2024;10(9):e30402.
11. Wang L, Li B, Dionysiou DD, Chen B, Yang J, Li J. Overlooked formation of H2O2 during the hydroxyl radical-scavenging process when using alcohols as scavengers. Environ Sci Technol.

2022;56(6):3386–96.

12. Kim HY, Kim TH, Yu S. Photolytic degradation of sulfamethoxazole and trimethoprim using UV-A, UV-C and vacuum-UV (VUV). J Environ Sci Health Tox Hazard Subst Environ Eng. 2015;50(3):292–300.
13. Lei Y, Yu Y, Lei X, Liang X, Cheng S, Ouyang G, et al. Assessing the use of probes and quenchers for understanding the reactive species in advanced oxidation processes. Environ Sci Technol. 2023;57(13):5433–44.
14. Robl S, Wörner M, Maier D, Braun AM. Formation of hydrogen peroxide by VUV-photolysis of water and aqueous solutions with methanol. Photochem Photobiol Sci. 2012;11(6):1041–50.
15. Buxton GV, Greenstock CL, Helman WP, Ross AB. Critical review of rate constants for reactions of hydrated electrons, hydrogen atoms and hydroxyl radicals (•OH/O•$^{-}$) in aqueous solution. J Phys Chem Ref Data. 1988;17(2):513–886.
16. Neta P, Huie RE, Ross AB. Rate constants for reactions of inorganic radicals in aqueous solution. J Phys Chem Ref Data. 1988;17(3):1027–284.
17. Berruti I, Polo-López MI, Oller I, Flores J, Marin ML, Bosca F. Sulfate radical anion: laser flash photolysis study and application in water disinfection and decontamination. Appl Catal B Environ. 2022;315:121519.
18. Chu C, Yan Y, Ma J, Jin S, Spinney R, Dionysiou DD, et al. Implementation of laser flash photolysis for radical-induced reactions and environmental implications. Water Res. 2023;244:120526.
19. Fennell BD, Mezyk SP, McKay G. Critical review of UV-advanced reduction processes for the treatment of chemical contaminants in water. ACS Environ Au. 2022;2(3):178–205.
20. Zhang Y, Guo Y, Fang J, Guo K, Yu G, Wang Y. Characterization of UV/chlorine process for micropollutant abatement by probe compound-based kinetic models. Water Res. 2023;237:119985.
21. Zhu S, Dong B, Wu Y, Bu L, Zhou S. Degradation of carbamazepine by vacuum-UV oxidation process: kinetics modeling and energy efficiency. J Hazard Mater. 2019;368:178–85.
22. Metolina P, Teixeira ACSC. A comprehensive dynamic kinetic model for the UVC/H2O2 process: application to zinc bacitracin degradation in wastewater as a case study. Environ Sci Pollut Res Int. 2021;28(19):24150–66.
23. Vajda S, Rabitz H, Walter E, Lecourtier Y. Qualitative and quantitative identifiability analysis of nonlinear chemical kinetic models. Chem Eng Commun. 1989;83(1):191–219.
24. Song M, Wang J, Chen B, Wang L. A facile, nonreactive hydrogen peroxide ($H_2O_2$) detection method enabled by ion chromatography with UV detector. Anal Chem. 2017;89(21):11537–44.
25. Guo Y, Zhang Y, Yu G, Wang Y. Revisiting the role of reactive oxygen species for pollutant abatement during catalytic ozonation: the probe approach versus the scavenger approach. Appl Catal B Environ. 2021;280:119418.
26. Popov E, Mametkuliyev M, Santoro D, Liberti L, Eloranta J. Kinetics of UV-$H_2O_2$ advanced oxidation in the presence of alcohols: the role of carbon centered radicals. Environ Sci Technol. 2010;44(20):7827–32.

27. Zhu C, Zhu F, Dionysiou DD, Zhou D, Fang G, Gao J. Contribution of alcohol radicals to contaminant degradation in quenching studies of persulfate activation process. Water Res. 2018;139:66–73.
28. Gonzalez MG, Oliveros E, Wörner M, Braun AM. Vacuum-ultraviolet photolysis of aqueous reaction systems. J Photochem Photobiol C Photochem Rev. 2004;5(3):225–46.
29. Goldstein S, Aschengrau D, Diamant Y, Rabani J. Photolysis of aqueous $H_2O_2$: quantum yield and applications for polychromatic UV actinometry in photoreactors. Environ Sci Technol. 2007;41(21):7486–90.
30. Ilan YA, Rabani J, Henglein A. Pulse radiolytic investigations of peroxy radicals produced from 2-propanol and methanol. J Phys Chem. 1976;80(14):1558–62.
31. Chen Y, Li B, Ou H, Mohseni M, Wang WL, Chen B. Molar absorption coefficients of water components under vacuum ultraviolet light, implications for pollutant degradation: a review. Environ Chem Lett. 2025;23(6):1863–76.
32. Furatian L, Mohseni M. Influence of chloride on the 185 nm advanced oxidation process. Chemosphere. 2018;199:263–8.

# Figures

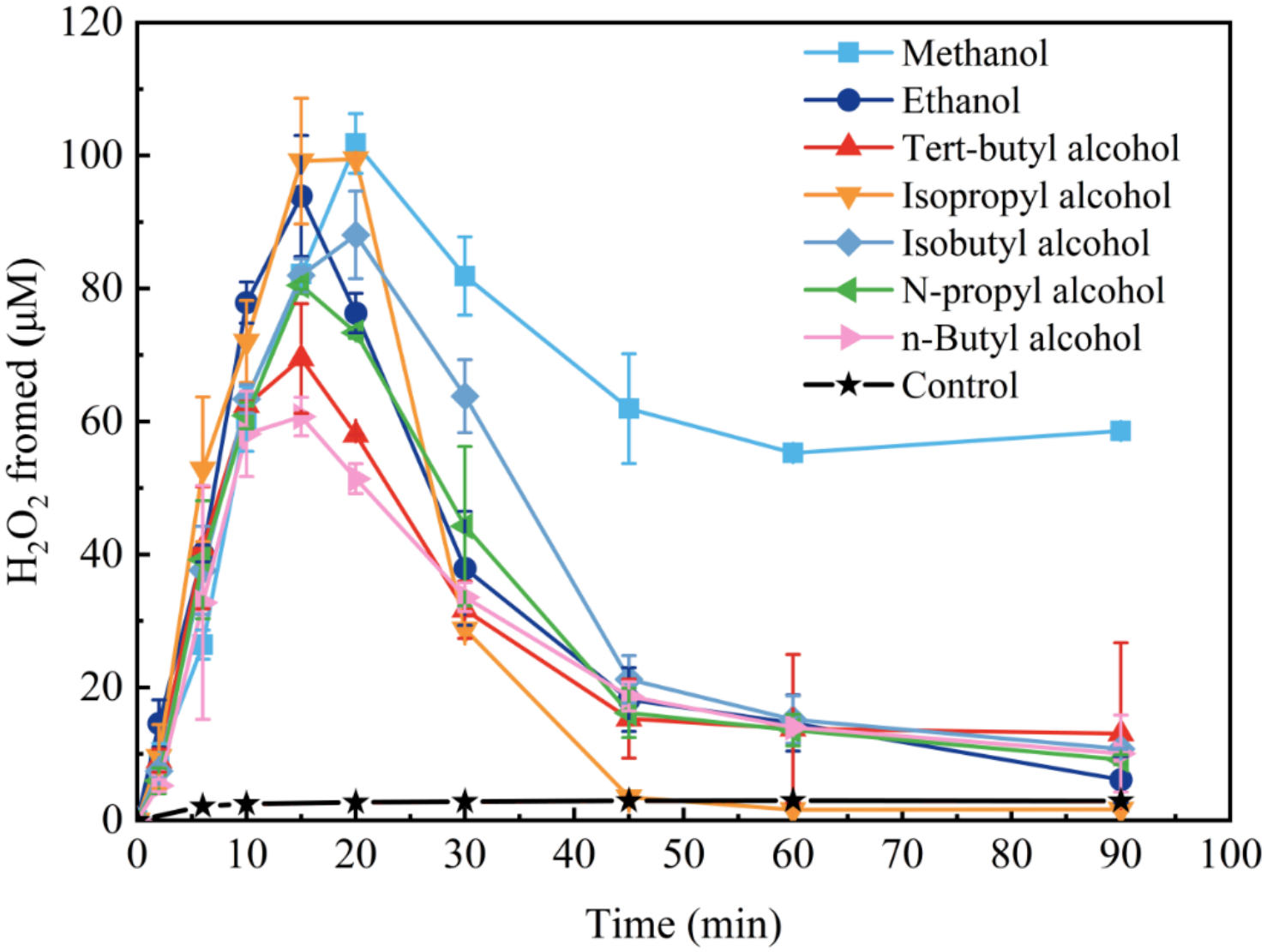



**Figure 1**

**Effects of alcohols on the formation and transformation of $H_2O_2$ during VUV/UV process. Reaction conditions: $[alcohols]_0$ = 1 mM, initial pH = 6.5 ± 0.3, temperature = 25 ± 0.1 °C, initial DO = 8.5 ± 0.5 mg/L. In the control experiment, each condition is the same except for absence of alcohols.**

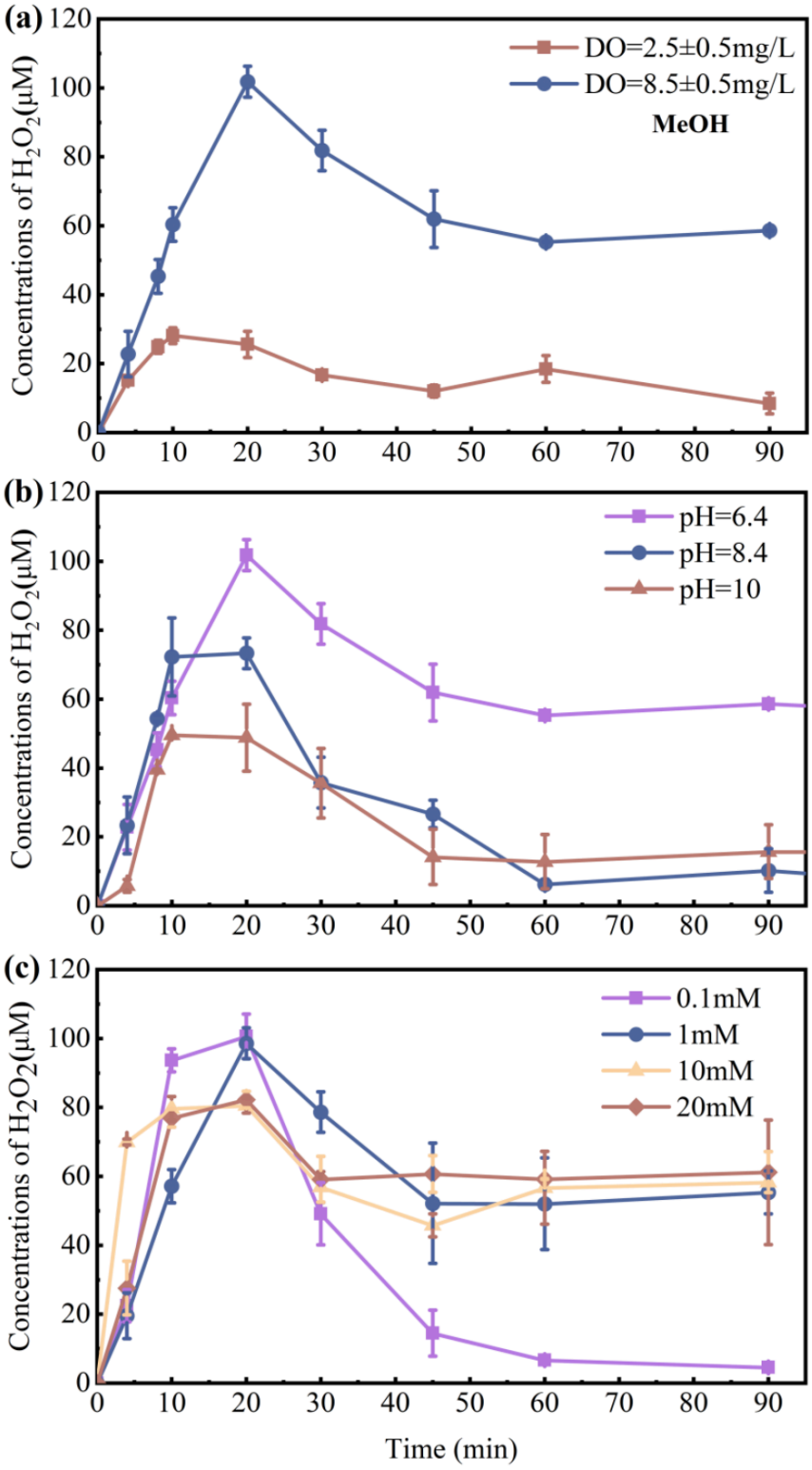



**Figure 2**

**Effects of DO (a), pH (b), and alcohol dosage (c) on the $H_2O_2$ evolution when dosing MeOH into the VUV/UV process ($[alcohols]_0$ = 1 mM, temperature = 25 ± 0.1 °C, initial DO = 8.5 ± 0.5 mg/L).**

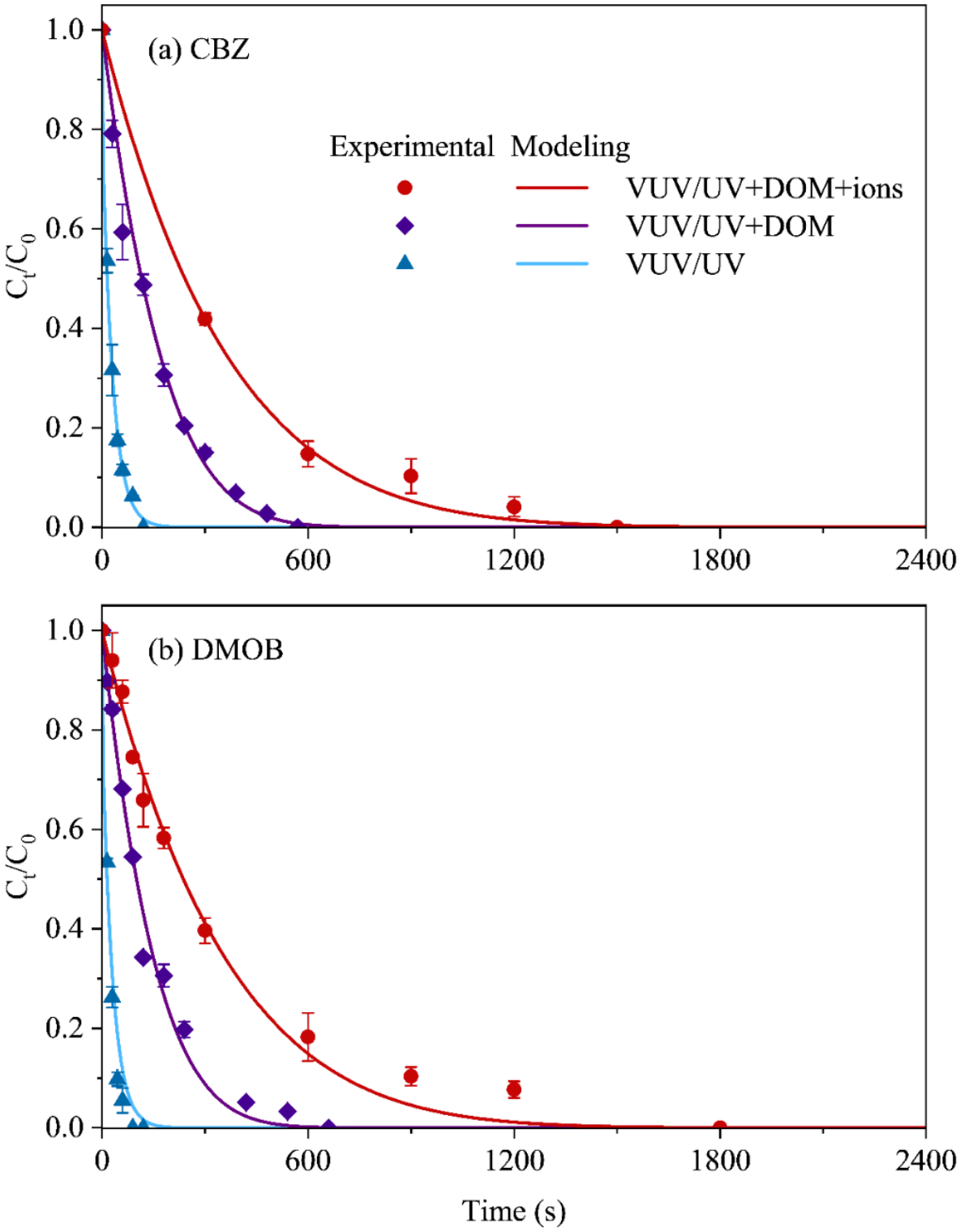



**Figure 3**

**Experimental and modelled degradations of (a) CBZ, and (b) DMOB in different reaction processes. Reaction conditions: [CBZ] = [DMOB] = 0.5 μM, [DOM] = 5.0 mg-C/L, [$Cl^-$] = 2 mM, [$Br^-$] = 10 μM, and [$HCO_3^-$] = 2 mM, initial pH = 7.5 ± 0.2, temperature = 25 ± 0.1 °C, initial DO = 8.5 ± 0.5 mg/L.**

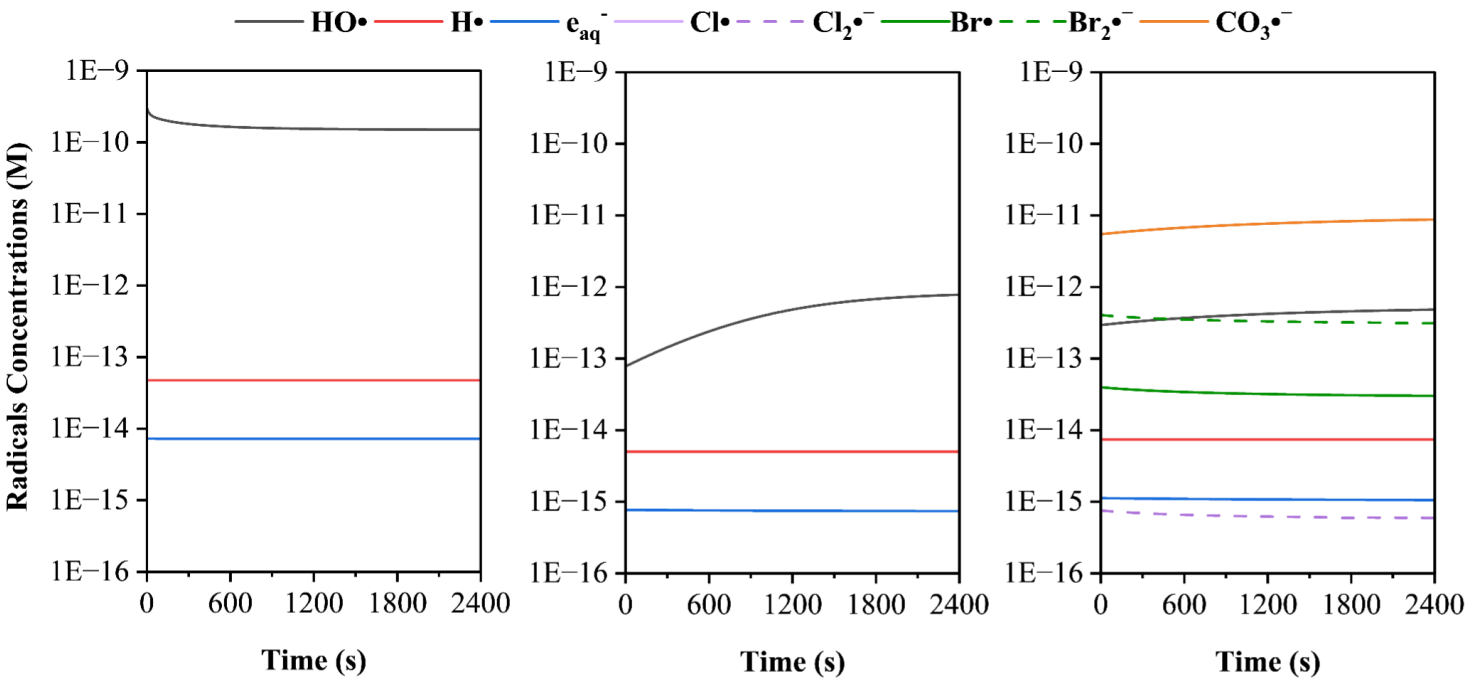



**Figure 4**

**Estimated radicals' concentrations in VUV/UV process of (a) pure water, (b) water containing 5 mg-C/L DOM only and (c) synthetic water containing DOM (5 mg-C/L), $Cl^-$ (2 mM), $Br^-$ (10 µM), and $HCO_3^-$ (2 mM). Reaction conditions: [NB] = 0.5 µM, initial pH = 7.5 ± 0.2, temperature = 25 ± 0.1 °C, initial DO = 8.5 ± 0.5 mg/L**

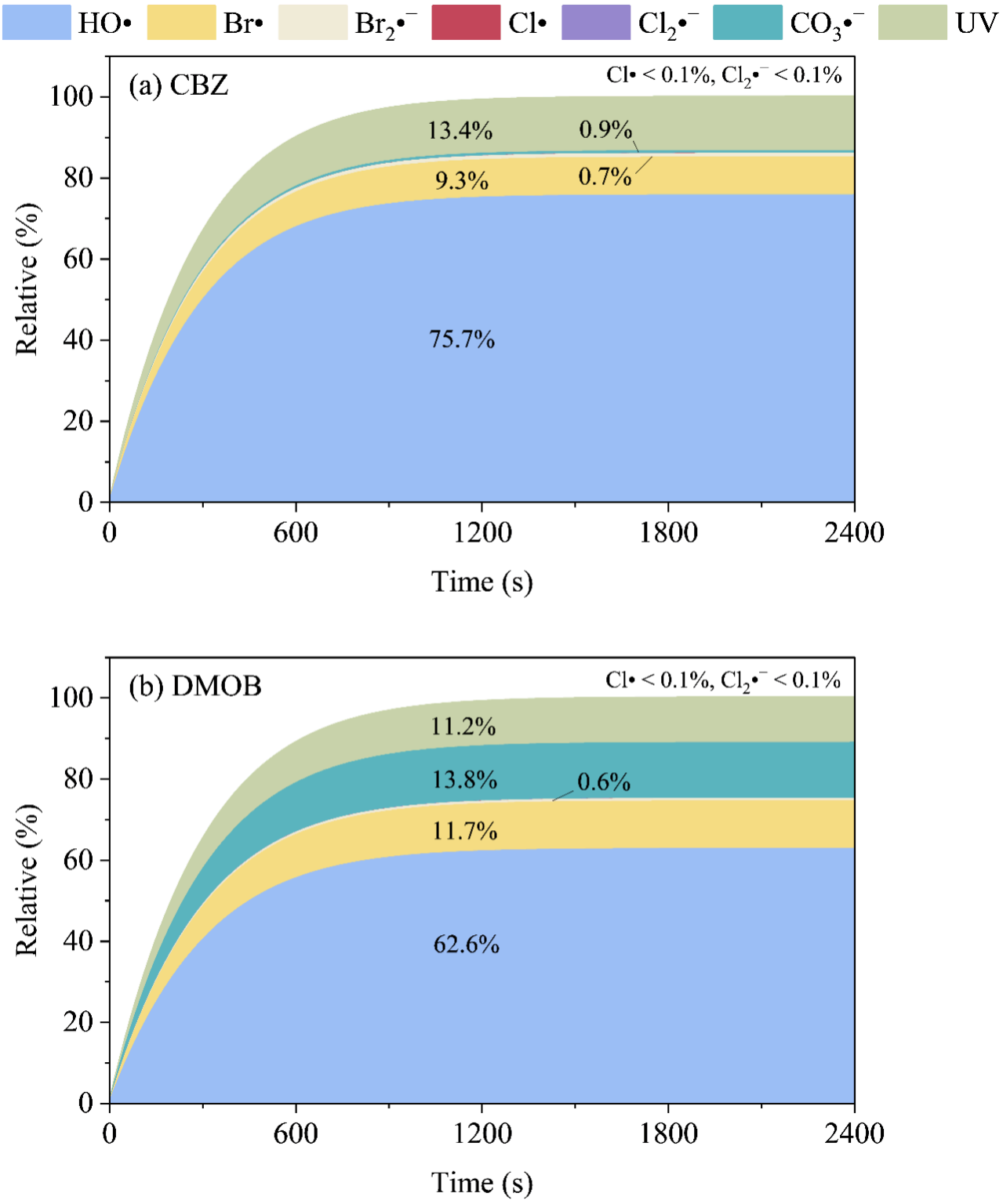



**Figure 5**

**Time-dependent cumulative contributions of HO•, Cl•, $Cl_2$•$^-$, Br•, $Br_2$•$^-$, $CO_3$•$^-$, and direct UV photolysis to the degradation of (a) CBZ and (b) DMOB during VUV/UV process in complex water. Reaction conditions: [CBZ] = [DMOB] = 0.5 μM, [DOM] = 5.0 mg-C/L, [$Cl^-$] = 2 mM, [$Br^-$] = 10 μM, and [$HCO_3^-$] = 2 mM, initial pH = 7.5 ± 0.2, temperature = 25 ± 0.1 °C, initial DO = 8.5 ± 0.5 mg/L.**

## Supplementary Files

This is a list of supplementary files associated with this preprint. Click to download.

- SupportingInformation.docx